

## Nanoscopic Pt Colloids in the “Embryonic State”

Klaus Angermund, Michael Bühl, Eckhard Dinjus, Uwe Endruschat, Franz Gassner, Heinz-Günter Haubold, Josef Hormes, Gesa Köhl, Frank Thomas Mauschick, Hartwig Modrow, Reinhard Mörtel, Richard Mynott,\* Bernd Tesche, Thomas Vad, Norbert Waldöfner, and Helmut Bönemann\*

It is generally accepted that when metal colloids are synthesized by wet chemical reactions, the first step is a reduction of the metal salt to give zerovalent metal atoms.<sup>[1]</sup> During the “embryonic stage” of the nucleation these atoms can collide in solution to form an irreversible “seed” of stable metal nuclei. Alternatively, the single metal atoms may be stabilized by complexation with ligands such as olefins and phosphanes, a process that is the basis of a rich organo-transition metal chemistry.<sup>[2]</sup> On repeating an old experiment for the formation of Ni colloids, published by Karl Ziegler in the context of the famous “nickel effect”<sup>[3,4]</sup> as early as 1954, we recently developed a novel, straightforward, general pathway to mono- and bimetallic nanoparticulates by the “reductive stabilization” of colloidal transition metals using trialkylaluminum compounds, which act both as reducing agents and as colloid stabilizers.<sup>[5]</sup> We now report that in the case of Pt we have been able to establish the mechanism of the colloid formation by a combination of NMR, ASAXS (anomalous small-angle X-ray scattering), XAS (X-ray absorption spectroscopy), DFT (density functional theory) computations, and electron microscopy.

When [Pt(acac)<sub>2</sub>] (**1**; acac = acetylacetonate) and AlMe<sub>3</sub> (**2**) react in toluene the reaction mixture turns from bright yellow to black over the course of about 24 h. <sup>1</sup>H NMR measurements were carried out in situ to monitor the reaction and to identify the products. In the initial <sup>1</sup>H NMR spectrum recorded about 30 min after the reagents had been mixed, a signal was observed at  $\delta = 0.51$  that is assigned to methyl groups in an intermediate platinum complex **3** on account of

the coupling with <sup>195</sup>Pt ( $I = 1/2$ , 33.8% natural abundance). Over the course of the next few hours this Pt–methyl signal became more intensive and at the same time the number of signals from other products increased (Figure 1).

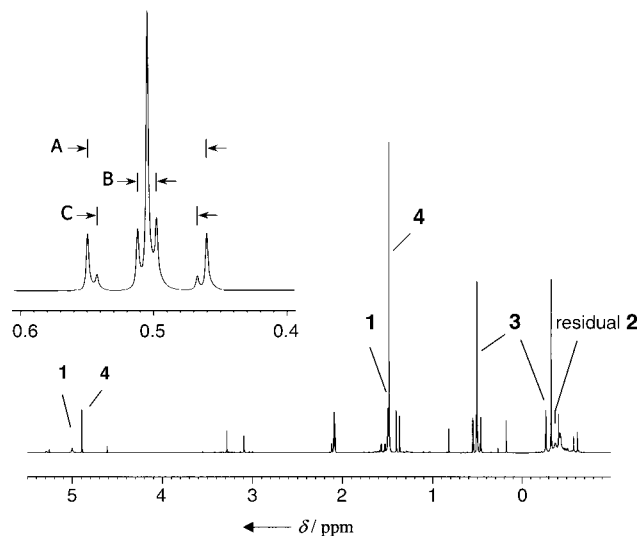


Figure 1. 400 MHz <sup>1</sup>H NMR spectrum of the mixture of **1** and **2** after 5 h at 27°C. The inset shows an expansion of the multiplet for the platinum-bound methyl group of **3** at  $\delta = 0.51$ . A:  $|^2J(^{195}\text{Pt}, ^1\text{H})| = 35.7$  Hz; B:  $|^4J(^{195}\text{Pt}, ^1\text{H})| = 5.7$  Hz; C:  $|^2J(^{195}\text{Pt}, ^1\text{H})| + ^4J(^{195}\text{Pt}, ^1\text{H})|$  (AA'X<sub>12</sub>X'<sub>12</sub> spin system, <sup>2</sup>J(<sup>195</sup>Pt, <sup>1</sup>H) and <sup>4</sup>J(<sup>195</sup>Pt, <sup>1</sup>H) have opposite signs).

The multiplet of the platinum-bound methyl group provides detailed information about the structure of the intermediate complex **3**. The intensity distribution is consistent with a binuclear platinum complex. The multiplet comprises the superimposed signals of isotopomers containing no <sup>195</sup>Pt nucleus (43.8%), one <sup>195</sup>Pt nucleus (44.8%), and two <sup>195</sup>Pt nuclei (11.4%); the latter is the most informative part of the signal and can be analyzed as the X region of an AA'X<sub>n</sub>X'<sub>n</sub> spin system (A = <sup>195</sup>Pt, X = <sup>1</sup>H). The complex must therefore be symmetrical but the platinum nuclei are not magnetically equivalent<sup>[6]</sup>—that is, the methyl groups must be terminal and not located in bridges between the platinum atoms. Furthermore, an exchange of the methyl groups between the platinum atoms on the NMR time scale can be ruled out.

EXAFS (extended X-ray absorption fine structure<sup>[7–11]</sup>) analyses were performed to obtain further insight into the structure of the intermediate complex **3** (Figure 2). The Fourier transform of **3** clearly differs from that of **1**, the analysis of which yields a Pt–O bond length of  $(2.00 \pm 0.01)$  Å in the first coordination shell, in agreement with previously published crystal structure data.<sup>[11]</sup> The detailed EXAFS analysis of **3** shows that the Pt absorber atom is directly surrounded by a light back scatterer, either C atoms at a distance of  $(2.11 \pm 0.02)$  Å or O atoms at a distance of  $(2.09 \pm 0.04)$  Å and Al atoms at a distance of  $(2.45 \pm 0.02)$  Å. Surprisingly no back scattering from Pt was observed, revealing that there is no Pt–Pt bond in the complex. This clearly indicates the existence of a bridging group between the two Pt atoms.

Evidence for a bridging group was obtained from a long-range COSY experiment (optimized for small H,H couplings).

[\*] Dr. R. Mynott, Prof. Dr. H. Bönemann, Dr. K. Angermund, Dr. M. Bühl, Dr. U. Endruschat, Dipl.-Chem. F. T. Mauschick, Dipl.-Chem. R. Mörtel, Dr. B. Tesche, Dr. N. Waldöfner  
Max-Planck-Institut für Kohlenforschung  
45466 Mülheim an der Ruhr (Germany)  
Fax: (+49) 208-306-2980  
E-mail: mynott@mpi-muelheim.mpg.de  
boennemann@mpi-muelheim.mpg.de

Prof. Dr. J. Hormes, Dr. G. Köhl, Dr. H. Modrow  
Physikalisches Institut  
Universität Bonn  
Nussallee 12, 53115 Bonn (Germany)

Prof. Dr. E. Dinjus, Dr. F. Gassner  
Forschungszentrum Karlsruhe  
Institut für Technische Chemie  
Postfach 3640, 76351 Karlsruhe (Germany)

Dr. H.-G. Haubold, Dr. T. Vad  
Forschungszentrum Jülich, Institut für Festkörperforschung  
52425 Jülich (Germany)

[+] Current address: Center for Advanced Microstructures and Devices  
Baton Rouge, FL 70806 (USA)

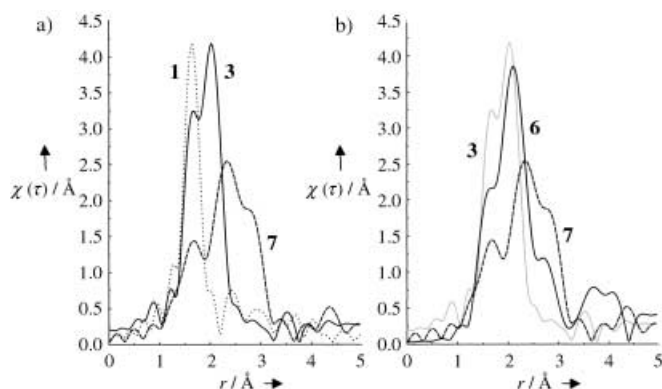
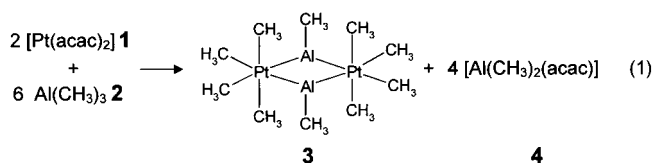


Figure 2. Fourier transform of Pt L<sub>III</sub> EXAFS signals. a) The intermediate complex **3**, [Pt(acac)<sub>2</sub>] (**1**), and the Pt colloid **7**. b) Pt particles **6** in solution, the intermediate complex **3**, and the Pt colloid **7**. The deviation between the distances displayed in the figure and the extracted distances in the material is due to the phase correction.

A cross peak was observed between the methyl signal at  $\delta = 0.51$  ppm and a singlet (no coupling to <sup>195</sup>Pt) at  $\delta = -0.27$  ppm in the region for aluminum-bound methyl groups. The integrated intensity of this resonance signal is one quarter of that of the platinum-bound methyl group. Further evidence was obtained when the complex was isolated from the reaction mixture. The pure complex **3** is rather unstable and decomposes rapidly in solution; however, in the presence of a fivefold excess of AlMe<sub>3</sub> it can be kept in solution for up to two days. Besides the signal for the platinum-bound methyl group, the <sup>1</sup>H NMR spectrum of **3** only shows the signal of the aluminum-bound methyl group at  $\delta = -0.27$  ppm, verifying that acetylacetonate can be excluded as a component of the bridge.

The spectra are consistent with the formation of a complex of structure **3** being formed in the initial stage of the reaction together with the aluminum acetylacetonate **4** [Eq. (1)]. Crystallographic data for a diiridium complex with bridging AlMe groups have been reported;<sup>[12]</sup> however, this is apparently the only literature reference to a binuclear transition metal complex with such bridging groups.



Further support for the unusual structure proposed for **3** is provided by density functional calculations (Figure 3). Starting from the proposed structure of **3**, the potential energy surface was explored at the BP86/ECP1 level of DFT.<sup>[13]</sup> The two most stable isomers that could be located are **3a** (*C*<sub>2v</sub> symmetry) and **3b** (*C*<sub>2h</sub> symmetry), both of which display four partially Pt–Al-bridging methyl groups. Isomer **3a** is the more stable, but **3b** lies only 1–2 kcal mol<sup>−1</sup> higher in energy. On searching for a transition state connecting **3a** and **3b**, a low-lying second-order saddle point **3c** (*C*<sub>2h</sub> symmetry) was located that is only 3.5 kcal mol<sup>−1</sup> above **3a**, indicative of a highly fluxional character for **3**. This saddle point would scramble all four methyl groups attached to one Pt atom, in

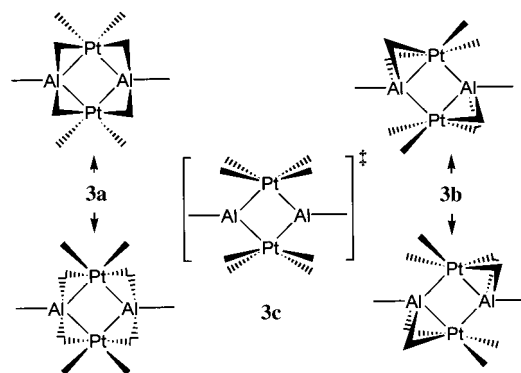


Figure 3. Results of the density functional calculations for the intermediate complex **3**.

accordance with the equivalence of these four groups on the NMR time scale. Isomers **3a** and/or **3b** are thus plausible candidates for the structure of **3** in solution.

Further experiments were performed to obtain more information on the way Pt atoms are formed from the complex **3**. Mass spectrometric analyses showed that [Pt(CH<sub>3</sub>)<sub>2</sub>(cod)] (**5**) is formed when the isolated complex **3** decomposes in solution in the presence of 1,5-cyclooctadiene (cod; see Scheme 1), which indicates that Pt(CH<sub>3</sub>)<sub>2</sub> fragments are likely to be the first step towards single metal atoms. The decomposition of Pt(CH<sub>3</sub>)<sub>2</sub> fragments by cleavage of the methyl groups is supported by the gas evolving during the colloid synthesis, which consists mainly of methane and small amounts of ethene and ethane.

The nucleation process was studied by time-resolved in situ ASAXS measurements for a reaction period of 1000 h.<sup>[14]</sup> Stable Pt particles **6** of 1.2 nm diameter were detected in solution after **3** had reacted for three days in the presence of **4** and an excess of **2**. The increase in the intensity of the small-angle scattering by almost an order of magnitude indicates the onset of cluster formation in the solution. Anomalous small-angle X-ray scattering was employed to confirm that the observed scattering arises from Pt particles. This method provides unbiased information on the distribution of the particle sizes even when there are significant contributions from other nanostructures.<sup>[15–17]</sup> These experiments show that the scattering arises from Pt particles with a diameter of 1.2 nm and with a rather narrow monomodal size distribution. Remarkably, the size remains unaltered during the course of the experiment (Figure 4a).

The increase in the mass fraction of Pt atoms transformed into particles (Figure 4b) is accounted for by the increase in

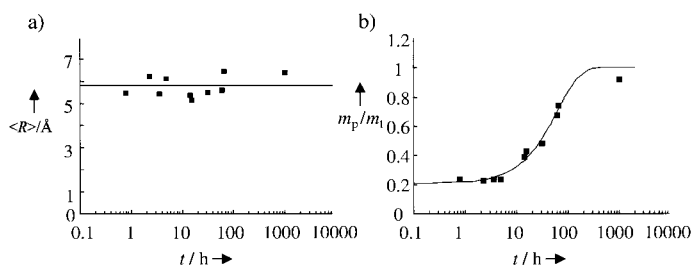


Figure 4. a) Time dependence of the mean particle radius  $\langle R \rangle$ , b) mass fraction  $m_p/m_t$  of Pt atoms transformed into particles ( $m_p$  = mass of platinum in particles,  $m_t$  total mass of platinum).

the number of these stable particles **6**. Complementary results are obtained by EXAFS. After four days in solution, Pt back scatterers at  $r = (2.71 \pm 0.1)^\circ\text{C}$  can be detected by Fourier analysis of the EXAFS data, proving that dissolved Pt particles **6** have been formed (Figure 2b).

The redispersible Pt colloid **7** can be isolated from the solution of the Pt nanoparticles in the form of a black solid. This colloid was investigated by a combination of high-resolution transmission electron microscopy (HRTEM), ASAXS, and XANES/EXAFS. The TEM images show that 1.2 nm globular Pt nanoparticles are present and that nearly all of the particles are amorphous, which was confirmed by optical Fourier transformation (Figure 5a). The particle size distribution is narrow and exhibits features of a monomodal log-normal distribution (Figure 5b).

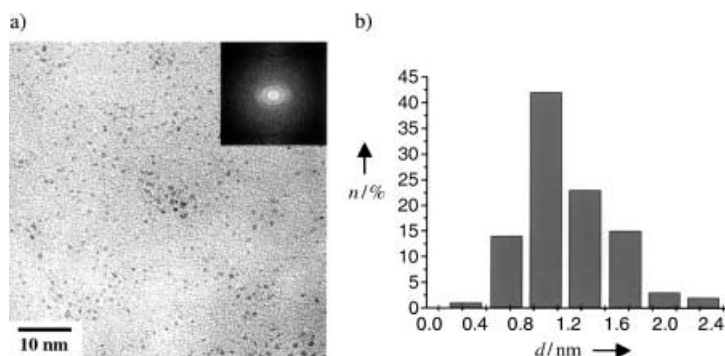


Figure 5. a) High-resolution transmission electron micrograph with optical diffractogram (Fourier transform) from different regions of the sample showing the amorphous character of the particles. b) Histogram of the particle size distribution.  $n$  = number of particles,  $d$  = particle diameter.

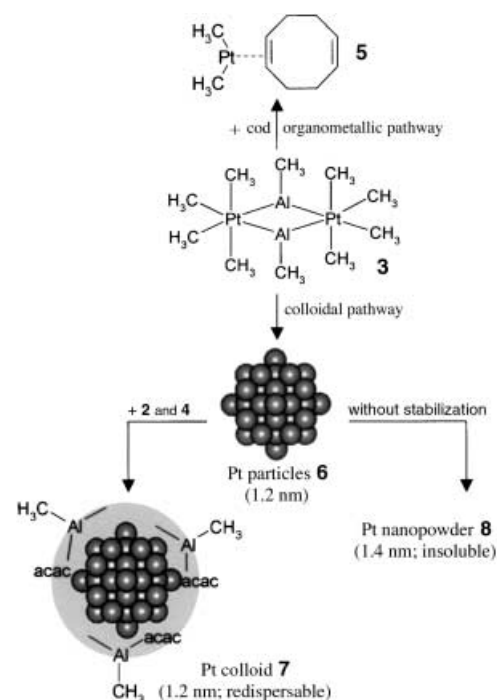
We conclude from these experiments that complexes of type **3** are general precursors from which organometallic complexes such as **5** can be synthesized by trapping reactions, or from which Pt nanoparticles such as **6** can be obtained by decomposition (Scheme 1).

In the presence of excess  $\text{Al}(\text{Me})_3$  (**2**) and  $[\text{Al}(\text{Me}_2)(\text{acac})]$  (**4**) a redispersible Pt colloid **7** (1.2 nm) can be isolated. When **3** decomposes in the absence of external stabilizers, a non-dispersible Pt nanopowder **8** with particles of 1.4 nm diameter is formed. The mean diameter is slightly greater than in the redispersible Pt colloid (**7**) as a result of agglomeration. Thus the products of the reaction between **2** and **4** act as a protecting shell which keeps the particles in solution. The reactivity of this protecting shell is a prerequisite for using the colloids **7** as building blocks for Pt nanoparticle networks.<sup>[18]</sup>

### Experimental Section

For the in situ experiments  $[\text{Pt}(\text{acac})_2]$  (60 mg, 0.15 mmol) was dissolved in  $[\text{D}_8]\text{toluene}$  (5 mL) under an argon atmosphere. A solution of  $\text{Al}(\text{CH}_3)_3$  (43.2 mg, 0.6 mmol) in  $[\text{D}_8]\text{toluene}$  (5 mL) was then added. After the solutions had been thoroughly mixed, the reaction mixture was transferred to a sealed sample tube (e.g. NMR tube, capillary) and subsequently to the respective instrument for characterization (NMR, ASAXS, XAS).

The NMR measurements were carried out at 300 K in  $[\text{D}_8]\text{toluene}$  on a Bruker AMX 400 NMR spectrometer equipped with a 5 mm inverse probehead.



Scheme 1. Schematic representation of the synthetic pathways starting from the intermediate complex **3**.

The experimental setup and data analysis for the X-ray absorption measurements (XANES/EXAFS) carried out at ELSA (Bonn, Germany) are described elsewhere.<sup>[7]</sup> A specially designed liquid cell similar to the one described in reference [8] was used for the in situ measurements. The Pt  $L_{III}$  edge EXAFS data were analyzed by using the UWXAFS analysis package.<sup>[9]</sup>

ASAXS measurements were carried out at the JUSIFA beamline (<http://www.fz-juelich.de/iff/personen/H.-G.Haubold>) at the Hamburg Synchrotron Radiation Laboratory HASYLAB-DESY. To compensate for contributions from background scattering, additional measurements were performed at a second X-ray energy  $E_2 = 11\,543\text{ eV}$  close to the L3 X-ray absorption edge of the Pt atoms. At this energy, the squared atomic scattering amplitudes of the Pt atoms are reduced by about 10% by anomalous scattering<sup>[15–17]</sup> and consequently the scattering cross section of Pt structures becomes smaller, whereas background scattering contributions remain unaffected and can be subtracted.

Received: February 8, 2002  
Revised: June 20, 2002 [Z18682]

- [1] T. Leisner, C. Rosche, S. Wolf, F. Granzer, L. Wöste, *Surf. Rev. Lett.* **1996**, *3*, 1105.
- [2] *Comprehensive Organometallic Chemistry* (Eds.: F. G. A. Stone, G. Wilkinson), Pergamon, Oxford, **1982**.
- [3] K. Ziegler, *Brennst.-Chem.* **1954**, *35*, 321.
- [4] K. Fischer, K. Jonas, P. Misbach, R. Stabba, G. Wilke, *Angew. Chem.* **1973**, *85*, 1002; *Angew. Chem. Int. Ed. Engl.* **1973**, *12*, 943.
- [5] H. Bönnemann, R. M. Richards, *Eur. J. Inorg. Chem.* **2001**, 2460.
- [6] R. J. Abraham, *Analysis of High Resolution NMR Spectra*, Elsevier, Amsterdam, **1971**.
- [7] W. Vogel, P. Britz, H. Bönnemann, J. Rothe, J. Hormes, *J. Phys. Chem. B* **1997**, *101*, 11029.
- [8] E. S. Marcos, M. Gil, J. M. Martinez, A. M. Muñoz-Paéz, A. S. Marcos, *Rev. Sci. Instrum.* **1994**, *65*, 2153.
- [9] E. A. Stern, M. Newville, B. Ravel, Y. Yacoby, D. Haskel, *Phys. B* **1995**, *208/209*, 117.
- [10] F. James, Reference Manual Version 94.1, CERN Program Library Long Writeup D506, **1998**.
- [11] M. Kathoh, K. Miki, Y. Kai, N. Tanaka, N. Kasai, *Bull. Chem. Soc. Jpn.* **1981**, *54*, 611.

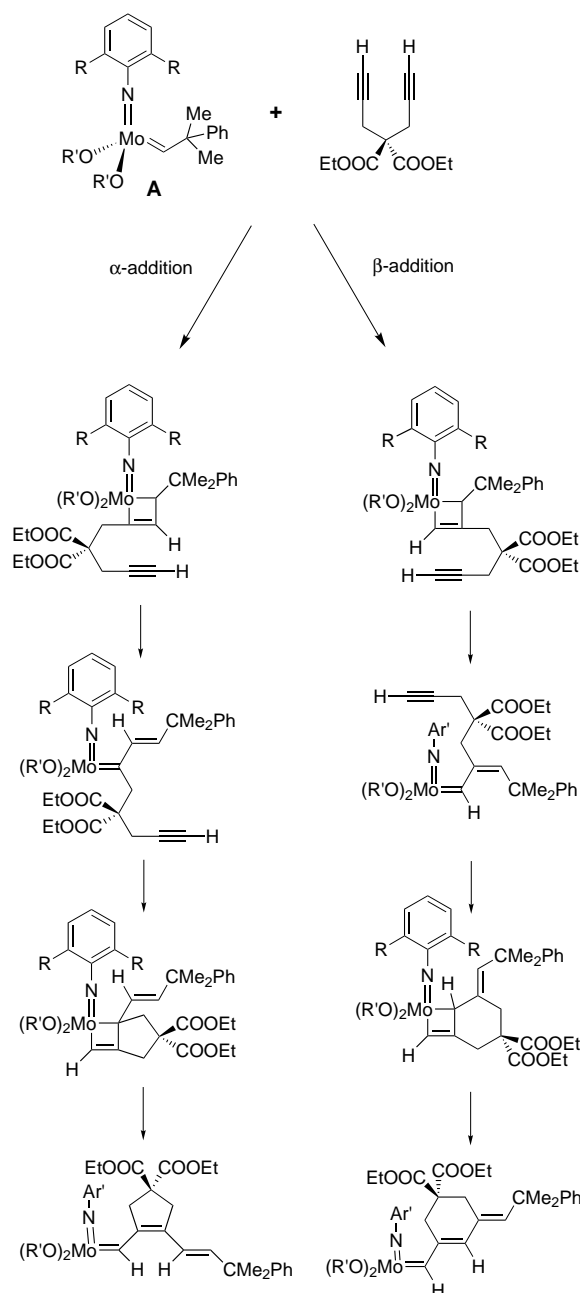
- [12] J. T. Golden, T. H. Peterson, P. L. Holland, R. G. Bergman, R. A. Andersen, *J. Am. Chem. Soc.* **1998**, *120*, 223.
- [13] For a description of the methods and the corresponding references see, for example: M. Bühl, S. Gaemers, C. J. Elsevier, *Chem. Eur. J.* **2000**, *6*, 3272; for a general assessment of density functional methods, see, for example: W. Koch, M. C. Holthausen, *A Chemist's Guide to Density Functional Theory*, Wiley-VCH, Weinheim, **2000**.
- [14] After preparation at the MPI in Mülheim, the samples were quenched to  $-78^{\circ}\text{C}$  and brought to the JUSIFA beamline where the measurements were performed at room temperature.
- [15] H.-G. Haubold, K. Grünhagen, M. Wagener, H. Jungbluth, H. Heer, A. Pfeil, H. Rongen, G. Brandenburg, R. Möller, J. Matzerath, P. Hiller, H. Halling, *Rev. Sci. Instrum.* **1989**, *60*, 1943.
- [16] H.-G. Haubold, X. H. Wang, H. Jungbluth, G. Goerigk, W. Schilling, *J. Mol. Struct.* **1996**, *383*, 283.
- [17] D. T. Cromer and D. A. Liberman, *Acta Crystallogr. Sect. A* **1981**, *37*, 267.
- [18] H. Bönemann, N. Waldöfner, H.-G. Haubold, T. Vad, *Chem. Mater.* **2002**, *14*, 1115–1120.

## Stereoselective Cyclopolymerization of 1,6-Heptadiynes: Access to Alternating *cis-trans*-1,2-(Cyclopent-1-enylene)vinylenes by Fine-Tuning of Molybdenum Imidoalkylidenes

Udo Anders, Oskar Nuyken,\*  
Michael R. Buchmeiser,\* and Klaus Wurst

Soluble, conjugated organic polymers are of great potential because of their intriguing optical and electronic properties.<sup>[1]</sup> Areas of interest include their use as conducting or semi-conducting polymers, organic light-emitting polymers, plastic solar cells, or more general, one or two-dimensional molecular wires. Any successful utilization depends on a high degree of definition as well as on the variability in the polymer structure. The cyclopolymerization of 1,6-heptadiynes containing suitable substituents at the 4-position offers an attractive access to polyenes with cyclic recurring units along the backbone.<sup>[2,3]</sup> The synthesis of such polymers requires the use of Ziegler-type catalysts,<sup>[4]</sup> Pd catalysts,<sup>[5]</sup> binary/ternary Mo- or W-based catalysts,<sup>[6]</sup> and anionic polymerization<sup>[7]</sup> Unfortunately, these methods lead to mostly insoluble, ill-

defined polymers, variable repeating units (i.e. 1,2-(cyclopent-1-enylene)-vinylenes and 1,3-(cyclohex-1-enylene)-methylidene), and broad molecular-weight distributions (polydispersity index (PDI)  $\gg 2$ ). However, well-defined high-oxidation-state Schrock-type molybdenum carbenes cyclopolymerize 1,6-heptadiynes in a living manner, yet result in polyenes that contain a mixture of five- and six-membered rings.<sup>[2,3,8]</sup> Usually these polymers display good solubility in common organic solvents (e.g.  $\text{C}_6\text{H}_6$ , toluene,  $\text{CH}_2\text{Cl}_2$ ,  $\text{CHCl}_3$ ), good long-term stability towards oxidation and high effective conjugation lengths ( $N_{\text{eff}}$ ).<sup>[2,3,9]</sup> The two different reaction pathways that are responsible for the formation of five- and six-membered ring structures are shown in Scheme 1.<sup>[2]</sup> The ring size of the polyene is influenced by steric and electronic effects of the ligands of the Schrock initiator **A**. Polymers



Scheme 1. Mechanisms for the cyclopolymerization of DEDPM with a Schrock-type initiator **A**.<sup>[2,3]</sup>

[\*] A. Univ.-Prof. Dr. M. R. Buchmeiser  
Institut für Analytische Chemie und Radiochemie  
Universität Innsbruck  
Innrain 52a, 6020 Innsbruck (Austria)  
Fax: (+43) 512-507-2677  
E-mail: michael.r.buchmeiser@uibk.ac.at  
Prof. Dr.-Ing. O. Nuyken, U. Anders  
Lehrstuhl für Makromolekulare Stoffe  
Technische Universität München  
Lichtenbergstrasse 4, 85747 Garching (Germany)  
Fax: (+49) 89-289-13562  
E-mail: oskar.nuyken@ch.tum.de  
Dr. K. Wurst  
Institut für Allgemeine, Anorganische und Theoretische Chemie,  
Universität Innsbruck  
Innrain 52a, 6020 Innsbruck (Austria)

Supporting information for this article is available on the WWW under <http://www.angewandte.org> or from the author.